Clim Dyn (2014) 43:911–924
DOI 10.1007/s00382-013-1909-3

Role of interaction between dynamics, thermodynamics and cloud microphysics on summer monsoon precipitating clouds over the Myanmar Coast and the Western Ghats

Siddharth Kumar · Anupam Hazra · B. N. Goswami

Received: 10 April 2013 / Accepted: 5 August 2013 / Published online: 18 August 2013

Abstract Indian summer monsoon circulation can be characterized by mean tropospheric temperature (TT) gradient between ocean and land. Two major heat sources, one near the Myanmar Coast and the other near the Western Ghats play seminal role in defining this TT gradient. While both regions are characterized by very similar orographic features, there are significant differences in frequency of occurrence of precipitating clouds and their characteristics even when the amount of rain in June–July months is almost same in the two regions. Deeper (shallower) clouds appear more frequently over the Myanmar Coast (the Western Ghats). There is a sharp decrease in amount of rainfall from June–July to August–September in both the areas. Rather counter intuitively, during the June–July–August–September season, low and moderate rains contribute more to the total rain in the Myanmar Coast while heavy rains contribute more to the total rain in the Western Ghats. Western Ghats also gets more intense rains but less frequently. With significant differences in moisture availability, updraft, amount and characteristics of cloud condensate in the two regions, this study proposes that the nontrivial differences in features between them could be explained by linkages between cloud microphysics and large scale dynamics. Presence of more cloud liquid water and the role of giant cloud condensation nuclei reveals dominance of warm rain process in the Western Ghats whereas more cloud ice, snow and graupel formation in the Myanmar Coast indicates stronger possibility of cold rain coming from mixed phase processes. Stronger heating caused by mixed phase process in the mid and upper troposphere in the Myanmar Coast and its feedback on buoyancy of air parcel explains the appearance of deeper clouds. Thus, our study highlights importance of mixed phase processes, a major cause of uncertainty in GCMs.

Keywords Summer monsoon · Microphysics · Dynamics · Latent heating · Aerosol

S. Kumar (✉) · A. Hazra · B. N. Goswami
Indian Institute of Tropical Meteorology, Dr. Homi Bhabha Road, Pashan, Pune 411 008, India
e-mail: siddharth.cat@tropmet.res.in

A. Hazra
e-mail: hazra@tropmet.res.in

B. N. Goswami
e-mail: goswami@tropmet.res.in

1 Introduction

Monsoon rainfall is the major driver of agricultural productivity in many tropical and subtropical regions of the world, and its variability affects the livelihood of a large share of the world's population (e.g. Parthasarathy et al. 1994). The Indian summer monsoon rainfall (ISMR), defined by the cumulative rainfall during June–July–August–September (JJAS) represents a major heat source in the tropical climate system. The ISMR is also responsible for several teleconnections influencing the climate around the world (Webster et al. 1998). While the ISMR represents a phase of the annual north–south march of the tropical convergence zone (TCZ), it is also influenced by the northward propagating monsoon intraseasonal oscillations (MISOs) with periodicity of about 30–60 days. One characteristic feature of seasonal mean monsoon rainfall is the two coastally oriented narrow rainfall maxima, one along the Western Ghats and the other along the Myanmar Coast. The location and intensity of these two precipitation maxima are results of interaction between the northward propagating MISO and the shallow orography in the two regions. The atmospheric response and teleconnections of

ISMR depend on the vertical structure of the heating associated with the heat source. As the vertical structure of different clouds (e.g. convective and startiform) are different, the resultant vertical structure of the mean heat source depends on the proportion of different cloud fractions (Tao et al. 2001) during the monsoon season. Therefore, better skill of seasonal mean prediction of ISMR would require climate models to simulate the different cloud fractions accurately during the monsoon season.

Despite the advances made in the development of climate models, dynamical forecast of ISMR remains a challenging problem (e.g. Sperber et al. 2001; Sperber and Palmer 1996; Webster et al. 1998; Wang et al. 2005; Kang and Shukla 2006). One reason for the difficulty in predicting ISMR by climate models is related to the fact that the potential limit on predictability of Asian monsoon is lower compared to that of other tropical climate systems (Goswami 1998; Goswami et al. 2006). The potential limit on predictability of seasonal mean is governed by relative contribution from predictable 'forced' component and unpredictable 'internal' component to the interannual variability (IAV) of the seasonal mean. The fact that 'internal' IAV arising from rectification of high frequency convective feedbacks in this region is as large as the contribution from the 'forced' variability (Goswami and Ajaya Mohan 2001) leads to a limit on the potential predictability of the Asian monsoon. Another difficulty in prediction of Asian monsoon arises due to the fact that the climate models are unsuccessful in simulating the observed distribution and intensity of monsoon rainfall with fidelity. The situation has not improved significantly from pre-CMIP3 models to CMIP3 models to CMIP5 models (Gadgil and Sajani 1998; Kang and Shukla 2006; Sperber et al. 2012). Why do models have such a hard time in simulating observed distribution and intensity of monsoon rainfall? The proportion of different types of clouds in this region is quite unique (Rajeevan and Srinivasan 2000; Romatschke and Houze 2011). We propose that the models' inability to simulate rainfall distribution is related to their inability to simulate the observed cloud fractions correctly (Slingo 1987; Walcek et al. 1990; Cess et al. 1990; Zhou et al. 2007). As the organized precipitation is a result of interaction between heating produced by the clouds and the induced circulation, errors in vertical structure (through errors in cloud types) could lead to larger biases in organized precipitation through such feedback. What then is the major cause of biases in simulating the cloud fractions in climate models? A complete description of precipitation formation requires a good understanding of the characteristics and behavior of the different hydrometeors in the atmosphere. Understanding the representation of some processes like auto conversion and accretion in the warm phase, aggregation and the Bergeron process in the mixed phase of the cloud formation are essential. We propose that the biases in representations of clouds in GCMs arise largely from inadequate representation of ice and liquid water content profiles (CIWC and CLWC) and integrated paths (CIWP and CLWP).

Winds interacting with orographic features can modulate processes of precipitation formation and growth mentioned above (Xie et al. 2006). Timescale for growth of cloud condensate and geometry of orography are closely linked (Houze 2012). Thus, interaction between background flow, orography and cloud microphysics [e.g., types and concentration of cloud condensation nuclei (CCN)] plays an important role in defining the two precipitation maxima mentioned earlier, one along the Western Ghats and another along the Myanmar Coast. However, to our knowledge, little exists in literature on how circulation and cloud microphysics interacts with orography in defining cloud types in these two areas. Therefore, we believe that these two regions provide the best test bed for studying this question. In an attempt to understand this interaction, the present study investigates the differences in the cloud types leading to precipitation in the two coastal regions and tries to unravel how these differences are related to differences in dynamic forcing and microphysical inputs for the clouds.

To set the background for our study of structure of rainfall and differences in cloud systems, Fig. 1a and b show JJAS mean rainfall spatial structure over region (50°E–120°E and 15°S–20°N) from two different data sets, Tropical Rainfall Measuring Mission (TRMM) from 1998 to 2010 and Global Precipitation Climatology Project (GPCP) from 1996 to 2009 respectively (Data description has been given in the next section). One can easily observe two regions of enhanced precipitation—one near the west coast of India and the other near the Myanmar Coast. We focus on regions highlighted by rectangular boxes shown in Fig. 1a. Three rectangular boxes in the left side represents the Western Ghats (72°E–74°E and 16°N–21.5°N, 73°E–75°E and 12°N–16°N, 74.5°E–76.5°E and 10°N–12°N) and the other three in the right side represents the Myanmar Coast (91°E–93.5°E and 18°N–22°N, 92°E–95°E and 16°N–18°N, 96°E–98.5°E and 10°N–16°N). Throughout this paper quantities averaged over these rectangular boxes are representative of these two regions of interest.

Annual cycle of rainfall shows similar rainfall amount in months of June and July near the Myanmar Coast and the Western Ghats (Fig. 1c), though the annual cycle of mean Outgoing Longwave Radiation (OLR) over these regions (Fig. 1d) indicates that the mean OLR over the Western Ghats is much higher than the Myanmar Coast. Mean rainfall in the two regions during June–July is similar in terms of magnitude although the spatial extent of rain is broader in the Myanmar Coast (Figs. 1c, 2a). But in August and September Myanmar Coast receives more rain than the Western Ghats (Fig. 2b). Observations suggest that even

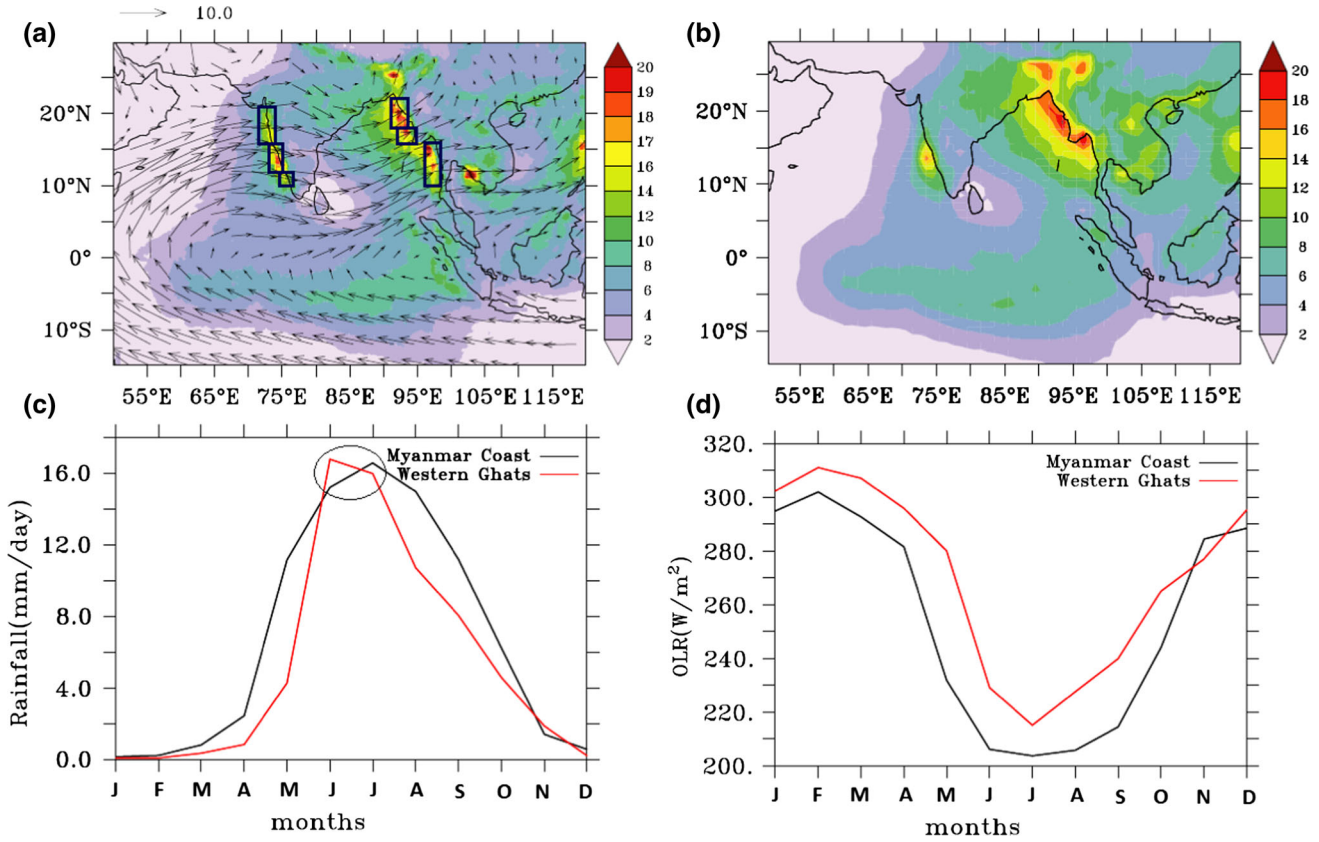

Fig. 1 **a** JJAS mean rainfall (mm/day) from TRMM and 850 hPa wind from ERA Interim (from 1998 to 2010). **b** JJAS mean rainfall (mm/day) from GPCP (from 1996 to 2009). **c** Annual cycle of rainfall averaged *over boxes* shown in Fig. 1a. **d** Annual cycle of OLR averaged *over boxes* shown in Fig. 1a

though precipitation amount is comparable in the two places during June–July, precipitation over the Western Ghats seems to come from shallower clouds compared to those over the Myanmar Coast. As OLR is related to the cloud top temperature, lower value of OLR is a manifestation of development of deeper cloud (with colder cloud top) whereas higher OLR represents shallower cloud (with warmer cloud top). Further the frequency of occurrence of OLR in different bins has been illustrated in Fig. 3. It is clear that low OLR (deeper cloud) appears much more frequently over the Myanmar Coast and high values of OLR (shallower cloud) appear more frequently over the Western Ghats. Having looked on the frequency of OLR one might ask the question: Why entirely different cloud systems in the two regions produce almost the same amount of rain? There is a sharp decrease in the amount of rain from June–July to August–September. But noteworthy feature is that the decrease in the amount of rain is much steeper in the Western Ghats than the Myanmar Coast.

To gain better insight into these differences in organization of cloud systems in the two regions, we analyze various satellite observations and some reanalysis products. On the basis of such analysis, we propose a hypothesis to explain these differences. We demonstrate that these differences may be attributed to atmospheric instability caused by cloud microphysics and its feedback to large scale dynamics. In Sect. 2 data set and methodology used for this study has been discussed. In Sect. 3 results and discussion has been given. Finally in Sect. 4, conclusion has been drawn.

2 Data and methodology

2.1 Rainfall and heating products

Tropical rainfall measuring mission (TRMM-3B42) data with 3-hourly temporal resolution and 0.25° by 0.25° spatial resolution in global belt from 50°S to 50°N from year 1998 to 2010 has been used to calculate the mean rainfall, Annual Cycle of rainfall, average number of heavy rainy days and percentage contribution of heavy, moderate and low rainfall and intensity of heavy rain (discussed in the next section). This data set is a combination of High Quality (HQ) microwave estimate and Variable Rain Rate (VAR) IR estimate which includes measurements from sensors

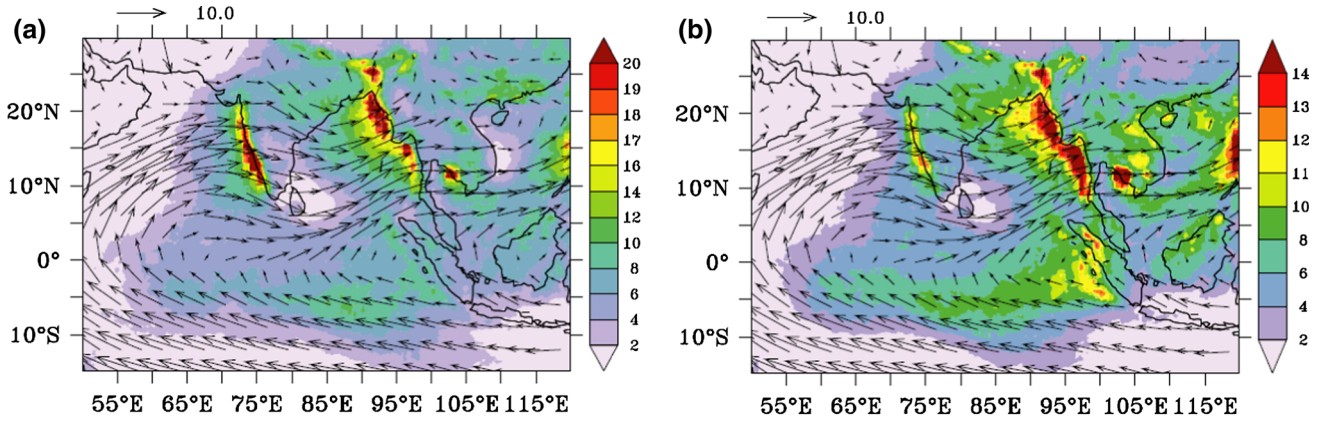

Fig. 2 **a** June–July mean rainfall (mm/day) from TRMM and 850 hPa wind from ERA Interim. **b** August–September mean rainfall (mm/day) from TRMM and 850 hPa wind from ERA Interim

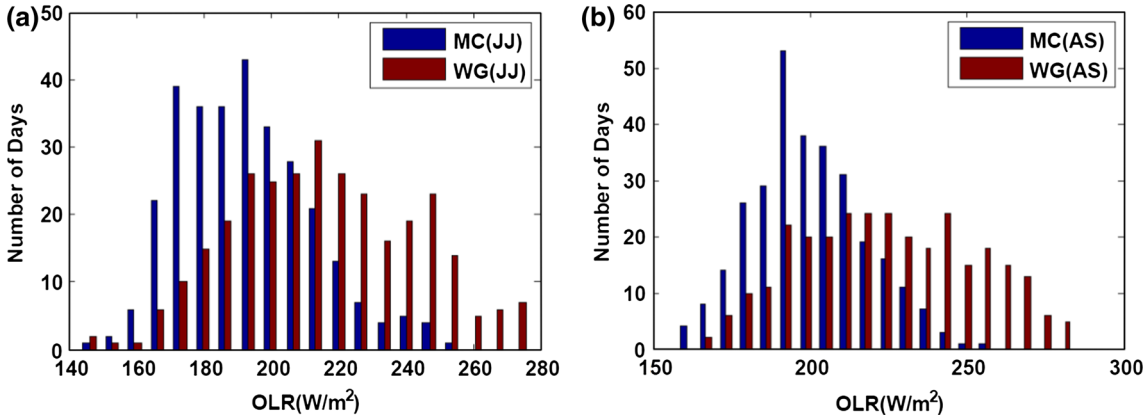

Fig. 3 **a** *Histogram* of OLR for June–July averaged *over boxes* shown in Fig. 1a. **b** *Histogram* of OLR for August–September averaged *over boxes* shown in Fig. 1a

TRRMM-TMI, Special Sensor Microwave Imager (SSM/I), Advanced Microwave Scanning Radiometer (AMSR) and Advanced Microwave Sounding Unit (AMSU). From available microwave data precipitation is estimated prior to use and then it is averaged to 0.25° by 0.25° spatial grids over time range ±90 min from nominal observation time. Two different infrared (IR) data sets are used for complete record of 3-hourly 0.25° by 0.25° gridded brightness temperatures. There is a simple approach named physically-based HQ estimate is used to combine HQ and VAR data sets. Detailed information about the data sets can be found on NASA website ftp:/meso-a.gsfc.nasa.gov/pub/trmmdocs/3B42_3B43_doc.pdf.

From three hourly datasets daily mean rain data has been prepared by taking means of all hourly rain data during any particular day. Rainfall has been categorized as heavy (above 40 mm/day), moderate (between 20 and 40 mm/day), and low (below 20 mm/day). Percentage contributions of heavy and low-moderate rain has been calculated by summing up all the rain events in respective category and dividing it by total rain at all grid point in JJAS season. All these quantities have been averaged over 13 years (1998–2010).

TRMM 3A25 (V7) data set (from 1998 to 2011)) has been used to calculate annual cycle of ratio of percentage of convective and stratiform rain (Meneghini et al. 1998; Meneghini and Jones 1993). This data set is aimed to compute various statistics on monthly basis from level 2 precipitation radar (PR) products. Unconditional convective and unconditional stratiform rain variables have been used for this purpose. Detailed description and algorithm involved can be found in recent work by (Pokhrel and Sikka 2012). GPCP (Global Precipitation Climate Project) daily data (2.5° by 2.5°, from 1996 to 2009) has also been used to calculate JJAS mean precipitation.

June–July and August–September mean latent heating profile (CSH heating from 1998 to 2009) has been calculated using convective stratiform heating profile from TRMM (Tao et al. 2006). Heating profile was derived from empirical relationships using a cloud resolving model.

There are 19 vertical levels and horizontal resolution is 0.5° by 0.5°.

TRMM 3A12 version-7 monthly data set (with 0.5° by 0.5° horizontal resolution, from 1998 to 2012) has been used to create monthly means of hydrometeors profiles. This data has been created from TRMM 2A12 data sets (Kummerow et al. 2001).

2.2 MODIS aerosol and cloud properties

MODIS level 3 version 5 monthly data (between 2003 and 2011) MYD 08 has been used to calculate annual cycle of aerosol optical depth. Aerosol optical depth at 550 nm has been used for present study (Kaufman et al. 1997; Kaufman and Tanré 1998). Terra and Aqua merged product MCD monthly products (from 2002 to 2011) have been used to calculate cloud liquid water path, cloud droplet effective radius, cloud ice and cloud ice effective radius. Variables such as cloud fraction and cloud top pressure uses linear averaging while making merged products from Terra and Aqua products. But for cloud Properties averaging is done on per pixel basis so that more number of observations with cloudy sky possesses more weightage in calculating monthly means.

2.3 AIRS and Kalpana INSAT

AIRS level 3 monthly products (AIRX3STM, from 2003 to 2011) with spatial resolution 1° by 1° have been used to calculate annual cycle of total precipitable water and OLR. These monthly mean values are arithmetic means of daily data. Quantities have been weighted by number of input counts per day in each grid box. All the parameters have been averaged and put in 1° by 1° grid boxes globally. Frequency of OLR has been calculated using Kalpana INSAT (Indian Satellite of Indian Space Research Organisation) 3-hourly OLR data from 2008 to 2012 after converting it to daily data.

2.4 CloudSat and MERRA

CloudSat daily products (from 2006 to 2008) have been used to calculate monthly mean vertical profiles of cloud condensate. Parameters are averaged over the rectangular boxes shown in Fig. 1a. On board radar on CloudSat provides high vertical resolution structure of clouds globally. For detailed description on CloudSat data one can look at recent paper by Rajeevan et al. (2012).

The Modern-Era Retrospective Analysis for Research and Application Analysis (MERRA) monthly product between 2001 and 2011 has been used to calculate mean vertical structure of cloud ice and cloud water present in the cloud anvil. Detailed description of data set is available in recent work (Rienecker et al. 2011). Annual cycle of Convective Available Potential Energy (CAPE) has been calculated using ERA Interim monthly means of daily means CAPE data from 2001 to 2010.

2.5 Design of the present study

All further analysis will be concentrated on rectangular boxes shown in Fig. 1a. Rectangular boxes in the Western Ghats cover regions: (72°E–74°E and 16°N–21.5°N, 73°E–75°E and 12°N–16°N, 74.5°E–76.5°E and 10°N–12°N) and boxes near the Myanmar Coast cover regions: (91°E–93.5°E and 18°N–22°N, 92°E–95°E and 16°N–18°N, 96°E–98.5°E and 10°N–16°N). Our main focus throughout this study will be Indian summer monsoon months (JJAS) only.

3 Results and discussion

We note from Fig. 1 that the seasonal mean rainfall (JJAS) is higher in the Myanmar Coast compared to that in the Western Ghats. How do different types of clouds (categories of rainfall) contribute to the seasonal mean? To gain insight to this question, we try to interpret the relative contribution of heavy, moderate and low rainfall to the seasonal mean rainfall. Contribution of different rain types to the seasonal mean rainfall over the two regions has been estimated and Fig. 4a–d show average number of heavy rainy days, percentage contribution of heavy rains, percentage contribution of low and moderate rains and intensity of heavy rains respectively during the JJAS season. In general heavy rainy events are caused by deeper clouds. Mean pattern of OLR and Cloud top Temperature also shows that OLR is low over the Myanmar Coast in summer monsoon months (not shown). This is consistent with the fact that frequency of occurrence of heavy rain is higher near the Myanmar Coast than the Western Ghats, agreeing with frequency of occurrence of low OLR showing relatively higher value in Myanmar Coast (Fig. 3). Although heavy rainfall events are more frequent near the Myanmar Coast, heavy rains contribute less to the seasonal mean rain compared to the Western Ghats that receives heavy rains less frequently (Fig. 4a, b). In other words low and moderate rain contributes more to the total rain in the Myanmar Coast (Fig. 4c). Numerical values of the percentage contribution of heavy, moderate and low rain to the seasonal mean rain is given in Table 1. Interestingly, average intensity of heavy rain is also higher in the Western Ghats though clouds appearing over this region are shallower (Fig. 4d and Fig. 3). These observations raise the following questions:

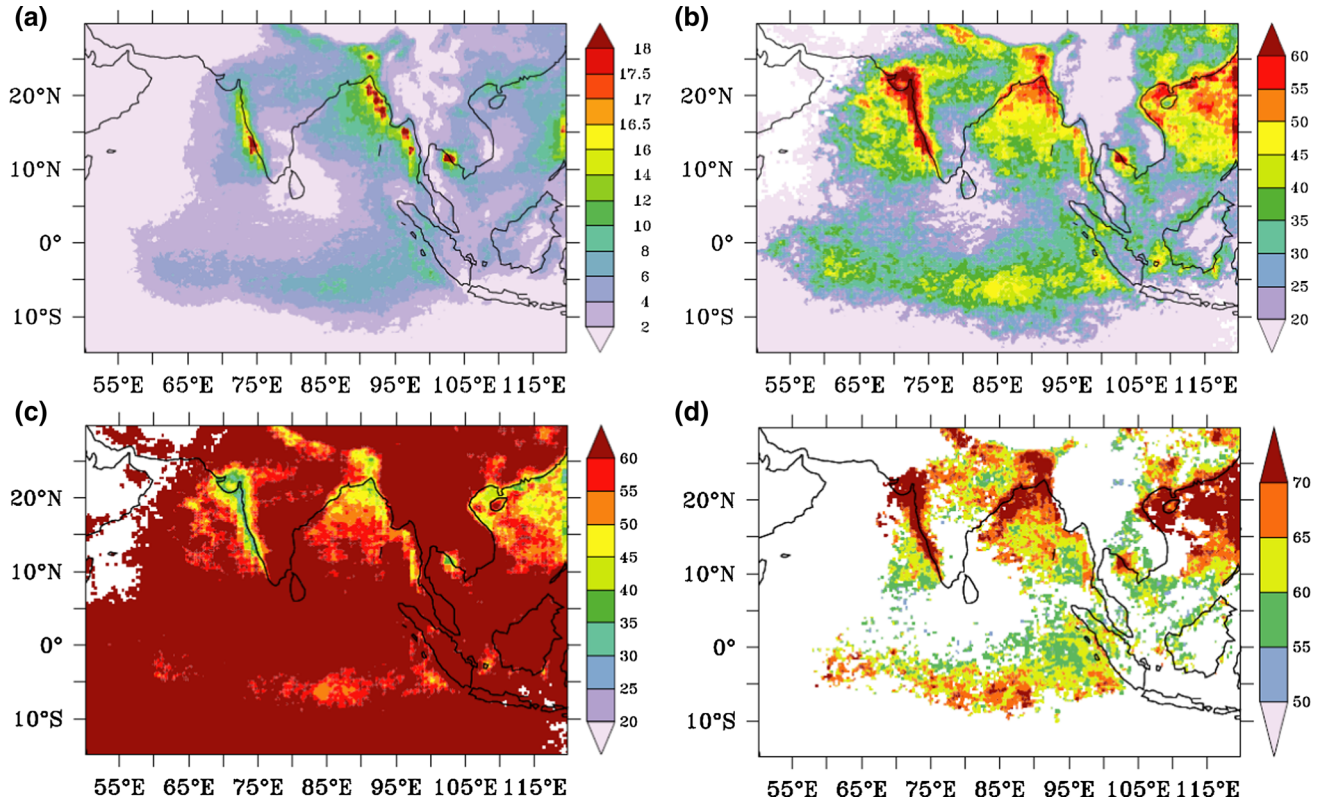

Fig. 4 **a** Average number of heavy rainy days. **b** Percentage contribution of heavy rain. **c** Percentage contribution of low plus moderate rain. **d** Intensity of heavy rain (mm/day per event)

Table 1 Percentage of three categories of rain rate (e.g., heavy (above 40 mm/day), moderate (between 20 mm/day and 40 mm/day), and low (below 20 mm/day)) in two different regions

Regions	% of heavy rain	% of moderate rain	% of low rain
Myanmar Coast	43.30	27.00	29.70
Western Ghats	57.17	22.53	20.30

1. Why is the frequency of deeper clouds always (throughout the monsoon season) higher in the Myanmar Coast compared to Western Ghats?
2. Even though frequency of deeper clouds is more in the Myanmar Coast, how can low and moderate rain events contribute more to the seasonal rainfall than the heavy rain events over this region?
3. What role does the microphysics play through cloud-aerosol interaction and feedbacks on large scale dynamics and on the precipitation over the two regions?

Our working hypothesis is that the last question is the key to understanding the striking differences in the precipitating clouds in the two regions. We try to arrive at some answers by analyzing a variety of satellite data sets and MERRA reanalysis.

3.1 Role of cloud microphysics in the precipitation formation processes

Interaction between aerosol and water vapor results in formation of clouds. Aerosol affects the formation of cloud droplets (in terms of number and size) (Twomey 1977; Twomey et al. 1984), cloud microphysical properties and finally precipitation processes. To investigate the role of microphysics due to aerosols, firstly we look at the total precipitable water and aerosol optical depth (AOD) (Fig. 5a, b). The figures indicate that the total precipitable water (Fig. 5a) is higher over the Myanmar Coast whereas AOD is less (Fig. 5b) compare to Western Ghats (June–July mean). Higher AOD in the Western Ghats may be attributed to advection of dust, sea salt aerosol due to long range transportation or local sources. Difference in aerosol loading prognosticates that interaction between cloud and aerosol may be critical in explaining substantial differences in cloud properties in these two regions. Figure 6a, b show annual cycle of column integrated cloud liquid water and cloud droplet effective radius respectively. It is noteworthy that the first indirect effect (smaller cloud drop size) and

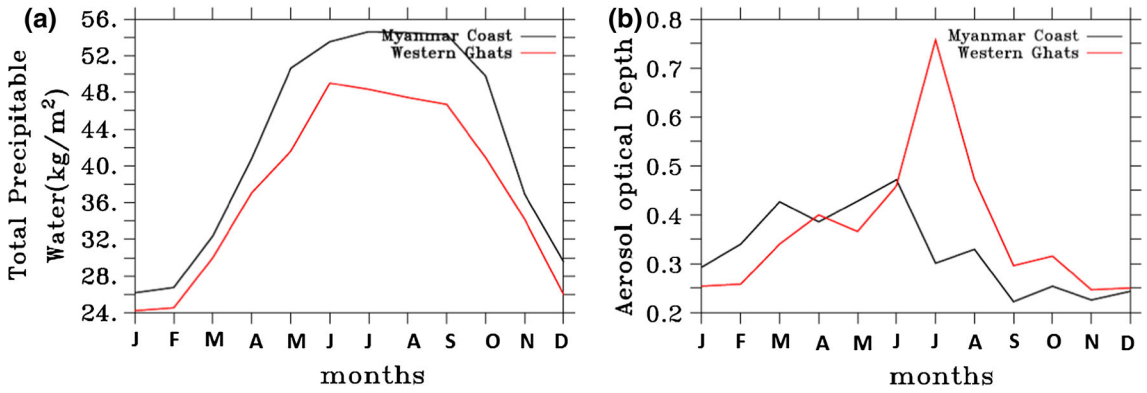

Fig. 5 **a** Annual cycle of total precipitable water averaged *over boxes* shown in Fig. 1a. **b** Annual cycle of aerosol optical depth averaged *over boxes* shown in Fig. 1a

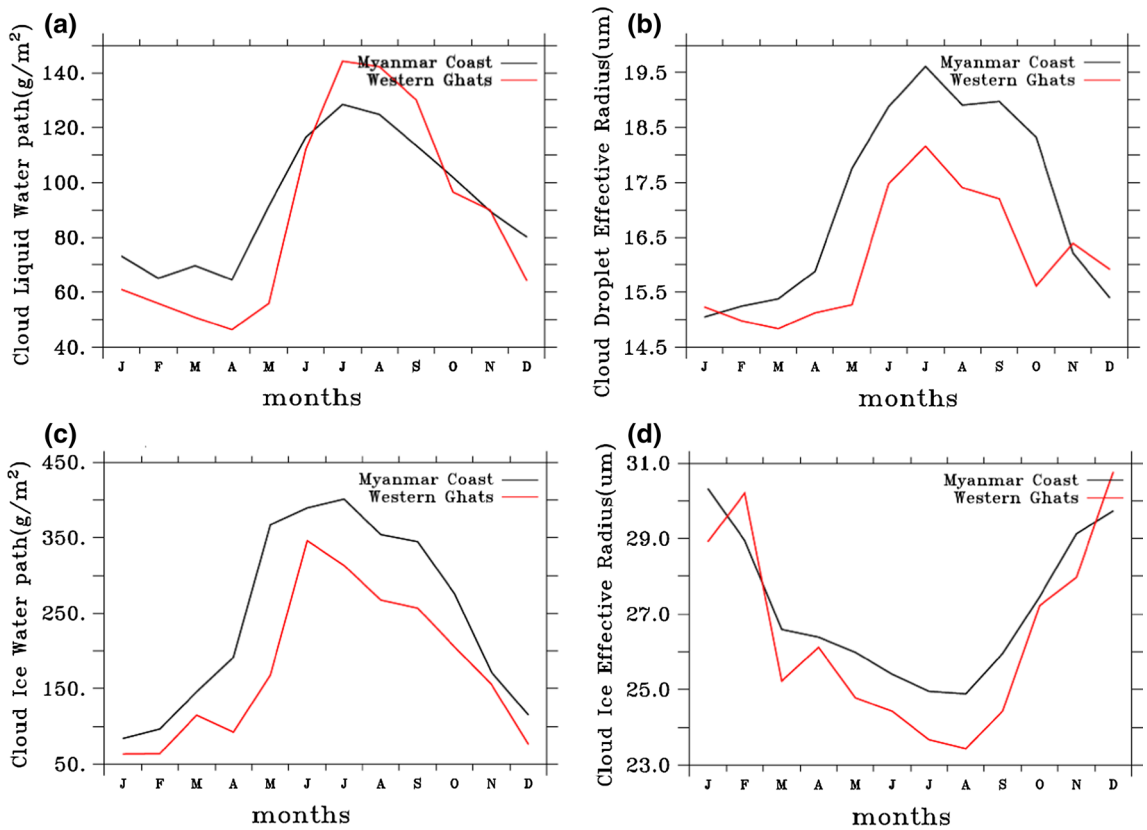

Fig. 6 **a** Cloud liquid water path averaged *over boxes* shown in Fig. 1a. **b** Cloud droplet effective radius averaged *over boxes* shown in Fig. 1a. **c** Cloud ice water path averaged *over boxes* shown in Fig. 1a. **d** Cloud ice effective radius averaged *over boxes* shown in Fig. 1a

second indirect effect (more cloud water, Twomey et al. 1984; Albrecht 1989) are well reflected over the two regions (Fig. 6a, b). For the same amount of water vapor available to cloud formation if the number of cloud droplets increases, their size decreases (Fig. 6b). This is mainly due to increase in the number concentration of cloud condensation nuclei (CCN). As the Western Ghats has more cloud water with smaller cloud drop size (Fig. 6a, b), it is unlikely to be able to produce more warm rain due to poor collision-coalescence efficiency (e.g., Squires and Twomey 1961; Warner and Twomey 1967; Warner 1968; Rosenfeld 1999). Interestingly higher cloud ice water path with higher cloud ice effective radius (Fig. 6c, d) appears over the Myanmar Coast compared to Western Ghats. Vertical structure of heating during June–July (Fig. 7a) and during August–September (Fig. 7b) in the two regions shows that while the heating maximum takes place at a higher altitude ($\sim$7 km) in the Myanmar Coast, the heating

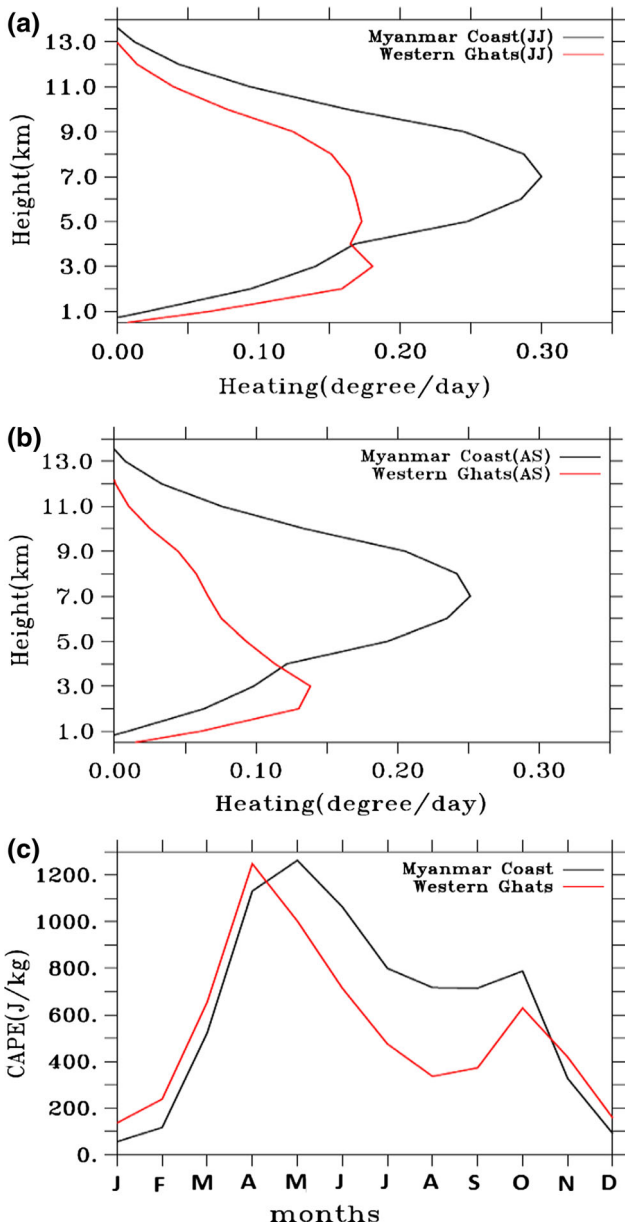

Fig. 7 **a** June–July mean latent heating averaged *over boxes* shown in Fig. 1a. **b** August–September mean latent heating averaged *over boxes* shown in Fig. 1a. **c** Convective available potential energy averaged *over boxes* shown in Fig. 1a

maximum in the Western Ghats is in the lower altitude (~4 km). Heating structure in the Western Ghats suggests stronger possibility of warm rain formation process as heating below 4 km would come primarily from latent heat release by condensation (where warm rain process occurs). However the exact cause of this behavior is difficult to decipher due to the complexity of the aerosol size distribution, but the presence of Giant Cloud Condensation Nuclei (GCCN) might account for this ambiguity. Major source of sea salt aerosol which acts as GCCN is the bursting of air bubbles near the sea surface. As winds are relatively stronger in the Arabian Sea during monsoon months, chances of formation of sea salt aerosol will be higher in the region near the Western Ghats (e.g., Satheesh and Krishnamoorthy 1997; Satheesh et al. 2001; Konwar et al. 2012). Smaller cloud droplets reside in the atmosphere for longer span of time because of lower fall speed. In the Western Ghats, at lower levels smaller cloud droplets keep on accumulating because of lower efficiency of collision coalescence, producing more cloud liquid water than the Myanmar Coast. Addition of some giant sea salt aerosol explains the production of more intense warm rain in the Western Ghats (Cheng et al. 2007; Khain et al. 2012) by directly activating the rain formation process through rain embryos (Fig. 4d). Another important phenomenon is the formation of rain through mixed-phase processes, which also controls the heating structure of mid and upper troposphere. As convective instability may help in formation of mixed phase precipitation and thereby influence the vertical structure of heating, we examine the background CAPE over the two regions (Fig. 7c). It is noted that during May–October CAPE is much higher in the Myanmar Coast compared to that in the Western Ghats.

The area averaged vertical profile of cloud liquid water content from CloudSat observation also shows higher value in the Western Ghats particularly at lower level (below 600 hPa, Fig. 8a, b) compared to the Myanmar Coast. From the point of view of cloud microphysics, smaller cloud droplets (over the Western Ghats) should evaporate faster leading to production of more water vapor (Tao et al. 2012). Therefore, the chances of formation of snow and graupel through vapor deposition process should get accelerated because of abundance of water vapor, but surprisingly the converse seems to be true in this case. One might ask the following questions: If cloud liquid water is more (over the Western Ghats), why not precipitation is higher? Secondly, why is the vertically integrated cloud ice (Fig. 6c) not higher in the Western Ghats? We believe that answers to these questions lie in the process of interaction among microphysics, thermodynamics and large-scale dynamics. It is shown that CAPE is relatively stronger in the Myanmar Coast compare to the Western Ghats (Fig. 7c) which eventually helps water vapor to be lifted to the freezing level (the height where freezing starts) (Fig. 8c, d). Thus water vapor in the Myanmar Coast reaches above the freezing level due to stronger updraft and produces more cloud ice through vapor deposition (Tao et al. 2012) although less cloud water is present at lower levels. The area averaged vertical profile of cloud ice content from CloudSat observation (Fig. 8c, d) also shows more cloud ice in the Myanmar Coast. Thus, although more cloud liquid water is present in the Western Ghats at lower level, it is not able to produces more cloud ice because of weaker updraft (low value of CAPE). Therefore one can

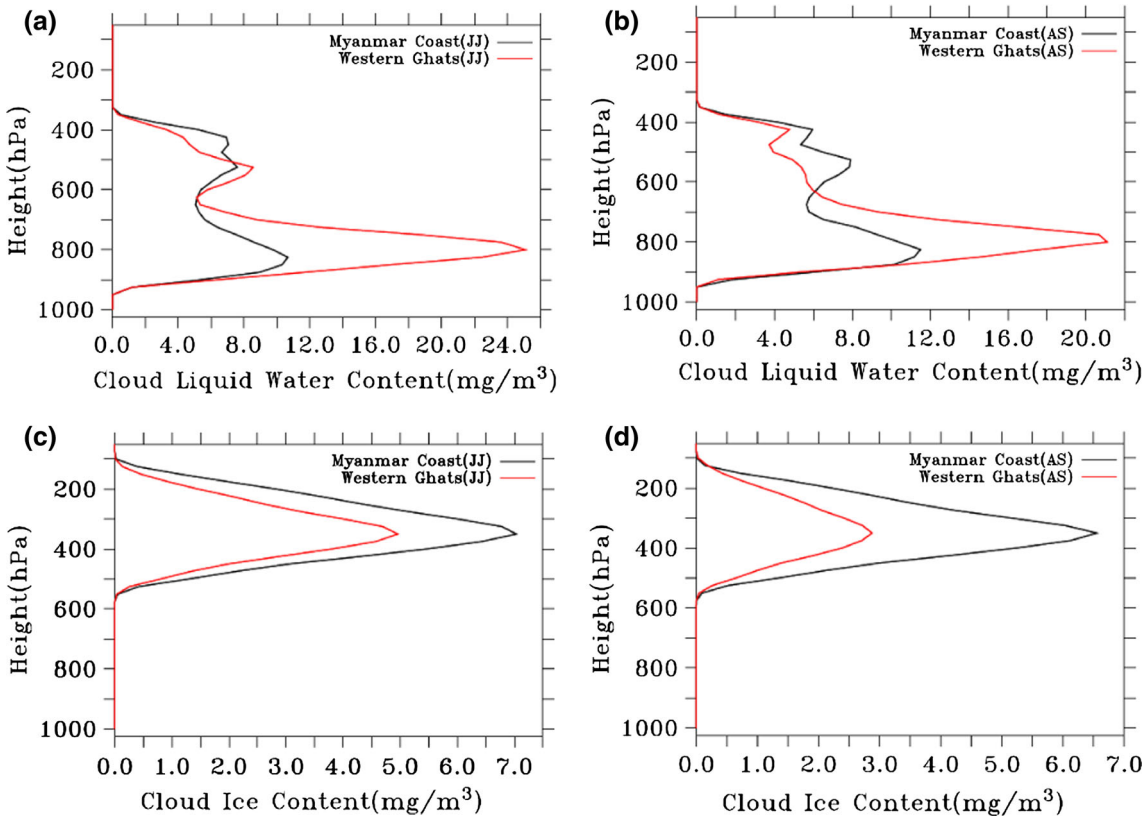

Fig. 8 **a** June–July mean cloud liquid water from CloudSat (mg/m^3) averaged *over boxes* shown in Fig. 1a. **b** August–September mean cloud liquid water from CloudSat (mg/m^3) averaged *over boxes* shown in Fig. 1a. **c** June–July mean cloud ice from CloudSat (mg/m^3) averaged *over boxes* shown in Fig. 1a. **d** August–September mean cloud ice from CloudSat (mg/m^3) averaged *over boxes* shown in Fig. 1a

conclude that there is a strong interplay between microphysics and dynamics in formation of hydrometeors.

Further, bigger cloud ice (Fig. 6d) over the Myanmar Coast results in a higher fall speed, which eventually forms mixed-phase hydrometeors (e.g., snow, graupel/hail) through auto-conversion from cloud ice (Cheng et al. 2010; Tao et al. 2012). Because of stronger updraft in the Myanmar Coast, vapor deposition of snow and graupel (mixed-phase) also seems to be higher. Riming processes of snow and graupel should also be higher in the Myanmar Coast due to higher cloud drop size (Fig. 6b, d) (Pruppacher and Klett 1997). Consequently we may argue that cold rain production (through snow and graupel melting) is more in the Myanmar Coast compared to the Western Ghats (Fig. 9). The TRMM observations also show that the Myanmar coast receives more stratiform rain fraction compared to the Western Ghats (Fig. 10a). On the other hand the percentage of convective rain (Fig. 10a) is higher in the Western Ghats. In a nutshell one can argue that warm rain process is dominant in the Western Ghats but cold rain coming from mixed phase process is dominant in the Myanmar Coast. As cold rain and warm rain process both contribute to the total rain, the total amount of rain in June–July is almost same in both the regions. In August and September although vertical structure of cloud condensate (cloud ice, cloud water) remains same, there is a sharp decrease in the amount in the Western Ghats (Fig. 10b, c), and hence a sharp decrease in the total rain (Fig. 2b).

3.2 Feedback process between cloud microphysics and dynamics

Latent heat release occurs in the mixed phase processes during the phase change (particularly due to microphysical conversion processes like deposition, accretion/riming, freezing, condensation). As these mixed phase processes are dominant in the Myanmar Coast, latent heat release in the mid and upper level will be stronger in that region (Fig. 7a, b). The striking difference in the vertical structure of latent heating in the two regions is crucial in understanding differences in the precipitating clouds as it can influence the dynamical response in a very significant way (Chattopadhyay et al. 2009). Enormous amount of latent heating provides a positive feedback to the buoyancy of air parcel and instability. Relatively intense heating in the Myanmar Coast (in the middle and upper levels),

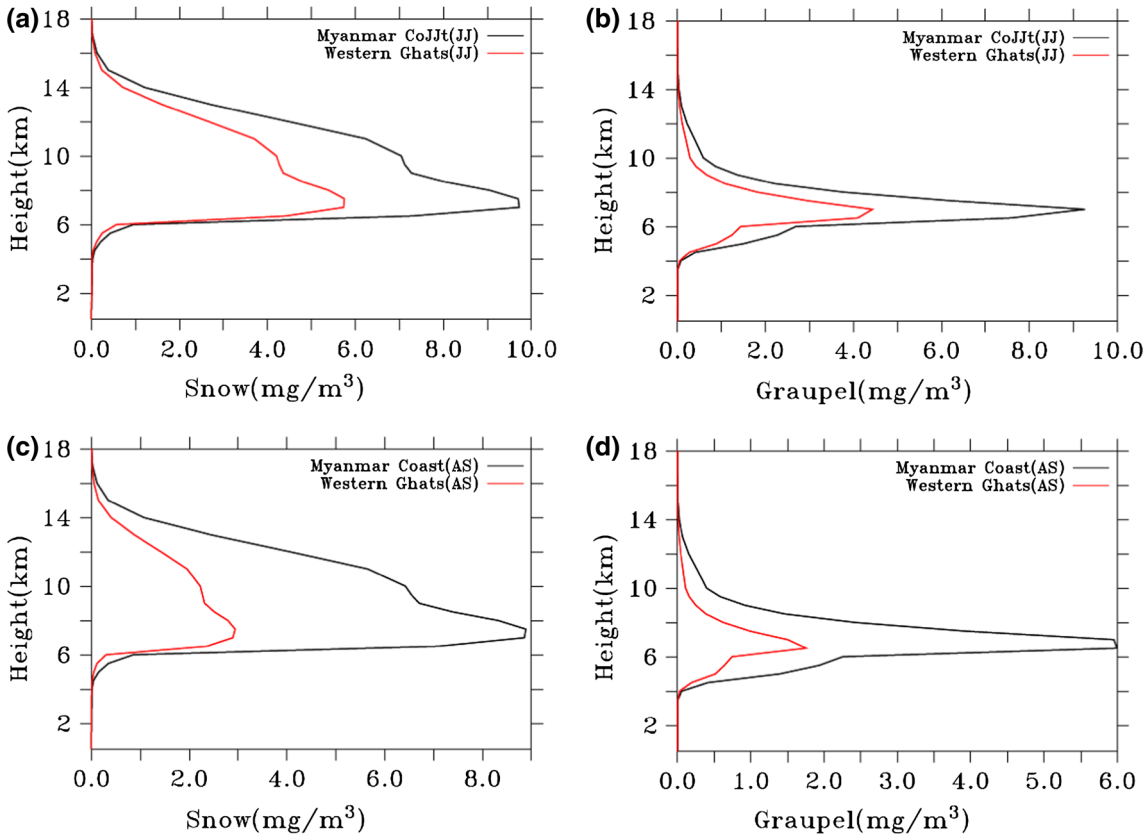

Fig. 9 **a** June–July mean snow from TRMM 3A12 (mg/m^3) averaged *over boxes* shown in Fig. 1a. **b** June–July mean graupel from TRMM 3A12 (mg/m^3) averaged *over boxes* shown in Fig. 1a. **c** August–September mean snow from TRMM 3A12 (mg/m^3) averaged *over boxes* shown in Fig. 1a. **d** August–September mean graupel from TRMM 3A12 (mg/m^3) averaged *over boxes* shown in Fig. 1a

strengthens updraft (through thermodynamic feedback) and the air parcel tends to lift up to much higher level forming deeper clouds (low OLR). This feedback clearly explains higher frequency of occurrence of low OLR in the Myanmar Coast (Fig. 3a, b). This heating structure affects large scale circulation by modulating the behavior of local convection centers. Positive feedback of latent heating also supports higher value of convective available potential energy in the Myanmar Coast (Fig. 7c).

3.3 Comparisons of the formation of cloud anvils for the two regions

This section is dedicated to explain issues related to percentage contribution of heavy, moderate and low rain in the entire JJAS season over the two regions of interest as discussed in last part of introduction. There is no significant difference in structure of cloud properties during June–July and August–September (except in magnitude). Therefore, arguments given in earlier sections (for June–July) holds true for entire JJAS season also. Higher instability in the Myanmar Coast (arising from latent heat release) pushes air parcel till the tropopause. After reaching the stable tropopause, air parcel spreads and forms cloud anvils. Figure 11a–d show cloud ice and cloud liquid water respectively present in the cloud anvil from MERRA reanalysis. Clearly Myanmar Coast shows higher value of cloud ice and cloud liquid water (above about 600 hPa) present in the anvil (Fig. 11). Presence of anvil cloud liquid water in the mid troposphere is a result of mixed-phase processes (where riming, deposition, melting etc. all taking place simultaneously). Higher value of anvil cloud liquid water (coming from mixed phase processes) and cloud ice, qualitatively reconfirms stronger chances of formation of anvils in the Myanmar Coast (Fig. 12). Much broader anvils present in the Myanmar Coast also reveal greater spatial extent of rain bands in the Myanmar Coast. As rain making process through mixed phase and formation of extended cloud anvil is more conducive in the Myanmar Coast, percentage of low and moderate rain is expected to be higher (Fig. 4c).

Similarly as mixed phase processes are less conducive in the Western Ghats and also formation of cloud anvils are less likely, percentage of low and moderate rain is lesser. Lesser percentage contribution of low and moderate rain in the Western Ghats implies higher contribution of heavy

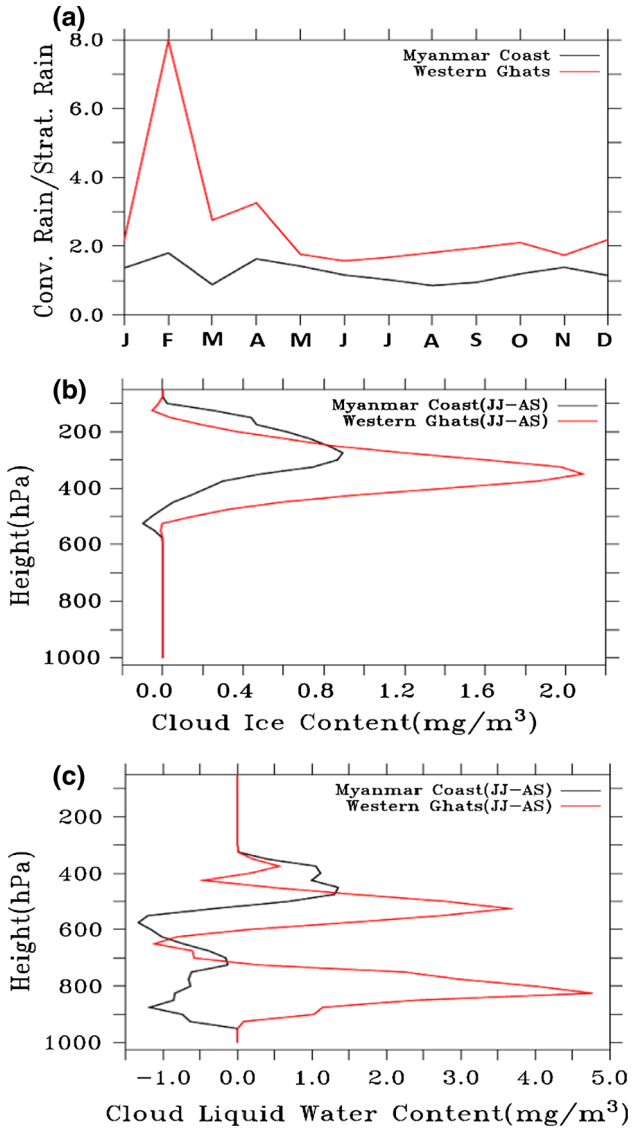

Fig. 10 **a** Ratio of convective and stratiform rain averaged *over boxes* shown in Fig. 1a. **b** Difference in cloud ice content in June–July and August–September averaged *over boxes* shown in Fig. 1a. **c** Difference in cloud liquid water in June–July and August–September averaged *over boxes* shown in Fig. 1a

rains. We recall that convective precipitation is characterized by heavy precipitation events with shorter spatio-temporal scale whereas stratiform rain is characterized by moderate rain events with broader spatio-temporal scale. Higher percentage of convective rain in the Western Ghats is a manifestation of larger contribution of heavy rain and similarly higher percentage of stratiform rain in the Myanmar Coast manifests into the larger contribution from low and moderate rain respectively. This result is consistent with earlier study carried out by Romatschke and Houze (2011) though there are differences in methodology of the classification of the convective and stratiform rain.

As discussed earlier clouds over the Western Ghats contain more cloud liquid water with smaller cloud drop size (Fig. 6a, b), resulting in poor collision-coalescence efficiency (e.g., Squires and Twomey 1961; Warner and Twomey 1967; Warner 1968; Rosenfeld 1999) and inefficiency to produce more warm rain. But addition of some giant sea salt aerosol acting as 'Rain Embryo' (Cheng et al. 2007) directly activate the rain formation process, resulting in the intense heavy rain events (Fig. 4d) over the Western Ghats although frequency of heavy rain is less (Fig. 4a).

4 Conclusion

There are significant differences in properties of clouds and rain formation process in the Western Ghats and the Myanmar Coast. Amount of precipitable water is more near the Myanmar Coast throughout the year and this area seems to be less polluted during summer monsoon months compared to Western Ghats. More amount of cloud liquid water with finer droplets appear over the Western Ghats but amount of ice and their effective radii shows smaller values. Higher value of convective available potential energy drives stronger updraft near the Myanmar Coast. These differences in precipitating clouds and rain formation process can't be explained by disjoint response of large scale dynamics, thermodynamics and microphysics. Role of aerosol in modulating large scale circulation through thermodynamics-microphysical feedback cannot be ignored. Marriage between cloud microphysics and large scale dynamics through latent heating feedback can explain most of the differences.

In the Myanmar Coast lower aerosol loading and more precipitable water gives rise to bigger cloud droplet but less in numbers whereas in the Western Ghats larger aerosol optical depth and less precipitable water results in smaller cloud droplet but more in numbers (Twomey Effect). Large number of smaller cloud droplets in the Western Ghats should suppress the rain formation process as efficiency of collision coalescence is lesser for smaller droplets. But giant cloud condensation nuclei coming from bursting of sea salt aerosol in the Arabian Sea enhances the warm rain process by directly activating rain formation. Smaller cloud droplet would also evaporate faster so availability of water vapor for the formation of snow through deposition process should be more. But on the contrary, in spite of smaller cloud droplets present in abundance in the Western Ghats, snow deposition is less likely because of weaker CAPE (updraft is much weaker and not enough of water vapor could be pushed above the height where freezing starts). Riming process is also less conducive because of lower values of cloud droplet effective radius and cloud ice effective radius.

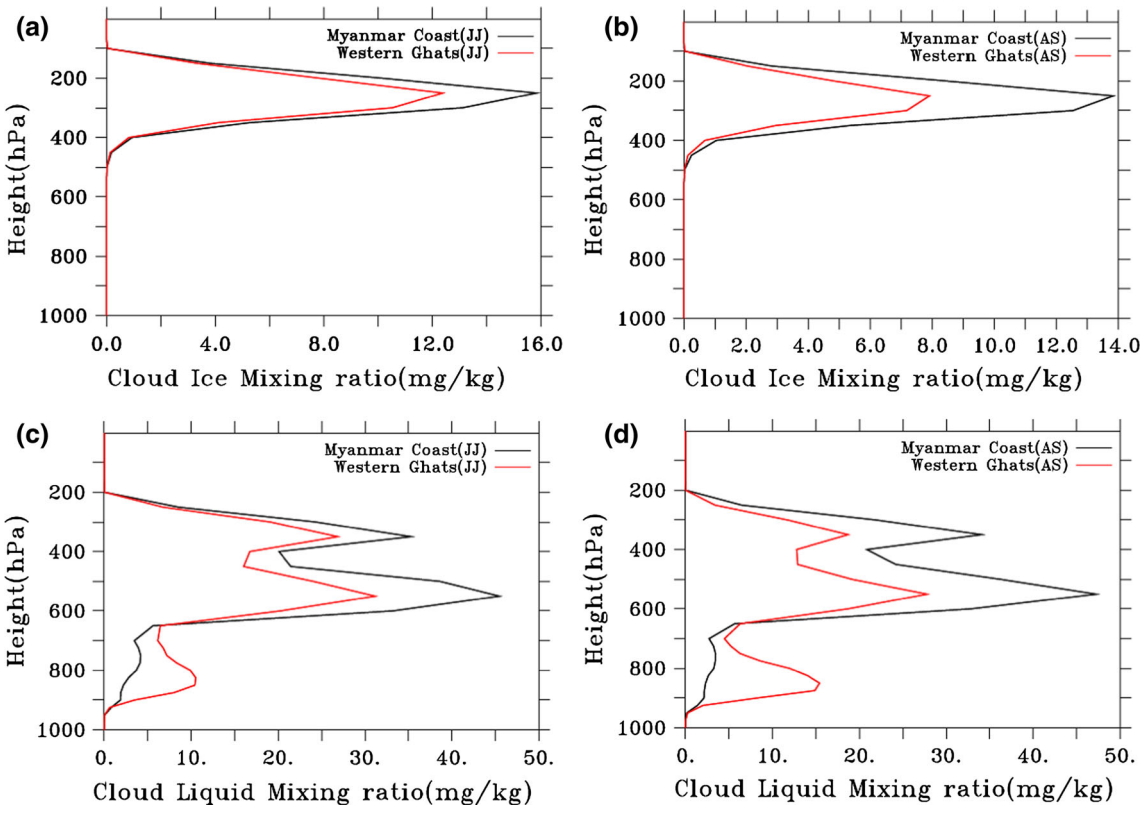

Fig. 11 **a** June–July mean cloud ice in anvil from MERRA (mg/kg) averaged *over boxes* shown in Fig. 1a. **b** August–September mean cloud ice in anvil from MERRA (mg/kg) averaged *over boxes* shown in Fig. 1a. **c** June–July mean cloud liquid water in anvil from MERRA (mg/kg) averaged *over boxes* shown in Fig. 1a. **d** August–September mean cloud liquid water in anvil from MERRA (mg/kg) averaged *over boxes* shown in Fig. 1a

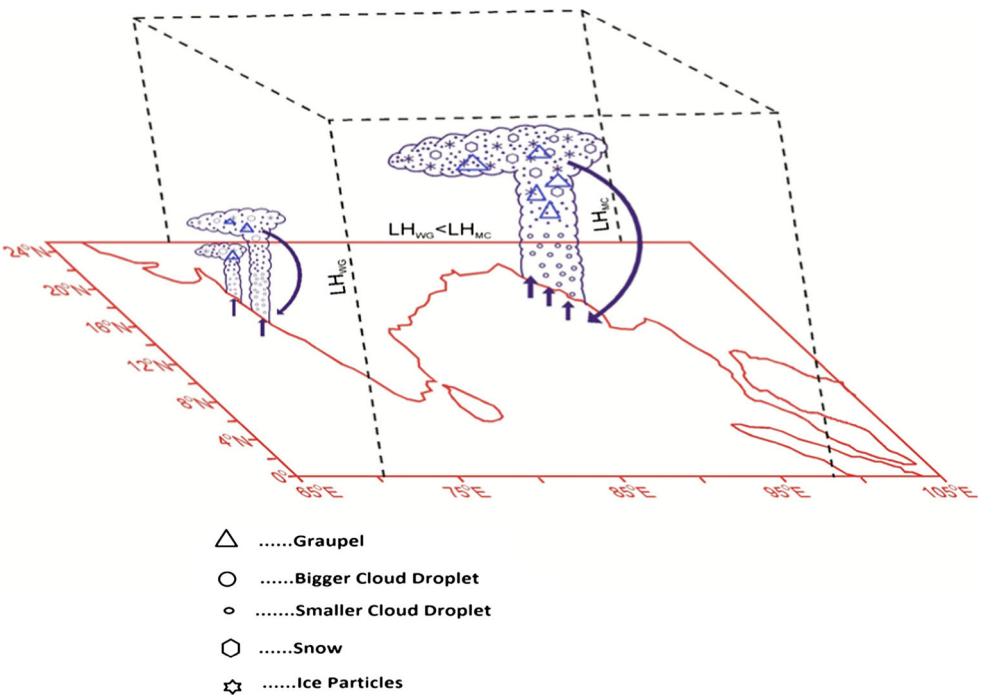

Fig. 12 Conceptual model of processes leading to differences in cloud organization system and precipitation over the Myanmar Coast and the Western Ghats

Bigger cloud droplets over the Myanmar Coast evaporate slowly and should reduce availability of water vapor for snow deposition process to take place. But less cloud liquid water available at lower levels implies stronger updraft tending to lift moisture below freezing temperature and hence improve the deposition process. Also bigger ice particles and bigger cloud droplets result in stronger possibility of riming process near the Myanmar Coast. Consequently condition for mixed phase processes (responsible for cold rain formation) is more favorable in the Myanmar Coast. Latent heating profile shows that lower level heating is stronger in the Western Ghats while mid and upper level heating are stronger in the Myanmar Coast. Lower level heating mainly comes from condensation and mid and upper tropospheric heating from mixed phase processes. Having analyzed the heating profile and conceptual framework for cloud and rain formation process, one can conclude that warm rain process is dominant near the Western Ghats and cold rain from mixed phase processes is dominant near the Myanmar Coast. Cumulative effects of warm and cold rain result in almost same amount of rain during June–July months over the two regions. Latent heating feedback on buoyancy of air parcel explains higher frequency of occurrence of low OLR over the Myanmar Coast (Fig. 12). The same argument is extended to explain percentage contribution of heavy, low and moderate rain in the two regions of interest. Much deeper clouds developing over the Myanmar Coast because of dynamical and latent heating response of the air column hits the tropopause and forms bigger cloud anvils. So, more than half of the rain comes from melting of snow and graupel present in the large scale and anvils of cloud. Generally low and moderate kind of rain occurs from these mixed phase process. That is why percentage contribution of low and moderate rain is more near the Myanmar Coast and less near the Western Ghats. In a nut shell, in this study, we unravel the importance of mixed phase processes in altering heating profile of the atmosphere resulting in a completely different type of response through dynamical feedback (Fig. 12).

The seminal role played by cloud microphysics through interaction with dynamics and thermodynamics in determining the precipitating clouds over the Asian monsoon region strengthens our hypothesis (see Sect. 1) that most biases in simulating precipitation over the Asian monsoon region by weather prediction and climate models are likely to be due to poor representation of cloud microphysics in these models. It highlights the urgent need to improve representation of cloud microphysics in their cloud parameterization schemes.

Acknowledgments Indian Institute of Tropical Meteorology (IITM), Pune, is fully funded by the Ministry of Earth Sciences, Government of India, New Delhi. Authors duly acknowledge NASA for the data sets TRMM, AIRS, MERRA etc. We also acknowledge the MODIS mission scientists and associated NASA personnel for the production of the data used in this research effort. Some data used in this study were produced with the Giovanni online data system, developed and maintained by the NASA GES DISC. Authors duly acknowledge Dr. X. Jiang of JPL, NASA for providing CloudSat data. Authors also sincerely thank Mr. M. Mahakur for providing OLR data from Kalpana Satellite and Mr. V. Sasane for helping in drawing the Schematic Diagram.

References

Albrecht BA (1989) Aerosols, cloud microphysics and fractional cloudiness. Science 245:1227–1230. doi:10.1126/science.245.4923.1227

Cess RD et al (1990) Intercomparison and interpretation of climate feedback processes in 19 atmospheric general circulation models. J Geophys Res 95:16601–16615

Chattopadhyay R, Goswami BN, Sahai AK, Fraedrich K (2009) Role of stratiform rainfall in modifying the northward propagation of monsoon intraseasonal oscillation. J Geophys Res 114:D19114. doi:10.1029/2009JD011869

Cheng C-T, Wang W-C, Chen J-P (2007) A modeling study of aerosol impacts on cloud microphysics and radiative properties. Quart J Roy Meteor Soc 133:283–297

Cheng C-T, Wang W-C, Chen J-P (2010) Simulation of the effects of increasing cloud condensation nuclei on mixed-phase clouds and precipitation of a front system. Atmos Res 96:461–476

Gadgil S, Sajani S (1998) Monsoon precipitation in the AMIP runs. Clim Dyn 14:659–689

Goswami BN (1998) Interannual variation of Indian summer monsoon in a GCM: external conditions versus internal feedbacks. J Clim 11:501–522

Goswami BN, Ajaya Mohan RS (2001) Intra-seasonal oscillations and inter-annual variability of the Indian summer monsoon. J Clim 14:1180–1198

Goswami BN, Wu G, Yasunari T (2006) Annual cycle, intraseasonal oscillations and roadblock to seasonal predictability of the Asian summer monsoon. J Clim 19:5078–5099

Houze RA, Jr (2012) Orographic effects on precipitating clouds. Rev Geophys 50:RG1001. doi:10.1029/2011RG000365

Kang I-S, Shukla J (2006) Dynamic seasonal prediction and predictability of the monsoon. In: B Wang (ed) The Asian monsoon, Ch. 15. Springer/Praxis Publishing Co., New York

Kaufman YJ, Tanré D (1998) Algorithm for remote sensing of tropospheric aerosol from MODIS. NASA MODIS Algorithm Theoretical Basis Document, Goddard Space Flight Center 85

Kaufman YJ, Tanre D, Remer LA, Vermote EF, Chu A, Holben BN (1997) Operational remote sensing of tropospheric aerosol over land from EOS moderate resolution imaging spectroradiometer. J Geophys Res 102:17051–17067

Khain AP, Phillips V, Benmoshe N, Pokrovsky A (2012) The role of small soluble aerosols in the microphysics of deep maritime clouds. J Atmos Sci 69:2787–2807

Konwar M, Maheshkumar RS, Kulkarni JR, Padmakumari B, Morwal SB, Deshpande CG, Axisa D, Burger R, Piketh S, Rosenfeld D, Goswami BN (2012) Contrasting polluted and pristine cloud microphysical properties over the Arabian Sea and Bay of Bengal. International conference on OCHAMP-2012, OC-000112

Kummerow C, Hong Y, Olson WS, Yang S, Adler RF, McCollum J, Ferraro R, Petty G, Shin DB, Wilheit TT (2001) The evolution of the Goddard profiling algorithm (GPROF) for rainfall estimation from passive microwave sensors. J Appl Meteor 40:1801–1840

Meneghini R et al (1998) Estimates of path attenuation for the TRMM radar. Geoscience and remote sensing symposium proceedings. IGARSS'98, IEEE International, 4 IEEE

Meneghini R, Jones JA (1993) An approach to estimate the areal rain-rate distribution from spaceborne radar by the use of multiple thresholds. J Appl Meteorol 32:386–398

Parthasarathy B, Munot AA, Kothawale DR (1994) All India monthly and seasonal rainfall series: 1871–1993. Theor Appl Climtol 49:217–224

Pokhrel S, Sikka DR (2012) Variability of the TRMM-PR total and convective and stratiform rain fractions over the Indian region during the summer monsoon. Clim Dyn. doi:10.1007/s00382-012-1502-1

Pruppacher HR, Klett JD (1997) Microphysics of clouds and precipitation. Kluwer Acad, Norwell

Rajeevan M, Srinivasan J (2000) Net cloud radiative forcing at the top of the atmosphere in the Asian monsoon region. J Clim 13(3):650–657

Rajeevan M, Rohini P, Niranjan Kumar K, Srinivasan J, Unnikrishnan CK (2012) A study of vertical cloud structure of the Indian summer monsoon using CloudSat data. Clim Dyn. doi:10.1007/s00382-012-1374-4

Rienecker MM et al (2011) MERRA: NASA's modern-era retrospective analysis for research and applications. J Clim 24:3624–3648. doi:10.1175/JCLI-D-11-00015.1

Romatschke Ulrike, Houze Robert A Jr (2011) Characteristics of precipitating convective systems in the South Asian monsoon. J Hydrometeorol 12(1):3–26

Rosenfeld D (1999) TRMM observed first direct evidence of smoke from forest fires inhibiting rainfall. Geophy Res Lett 26:3105–3108. doi:10.1029/1999GL006066

Satheesh SK, Krishnamoorthy K (1997) Aerosol characteristics over coastal regions of the Arabian Sea. Tellus 49B:417–428

Satheesh SK, Krishnamoorthy K, Das I (2001) Aerosol spectral optical depths over the Bay of Bengal, Arabian Sea and Indian Ocean. Curr Sci 81:1617–1625

Slingo A (1987) The development and verification of cloud prediction scheme for the ECMWF model. Q J Roy Meteorol Soc 113:899–927

Sperber KR, Palmer TN (1996) Interannual tropical variability in general circulation model simulations associated with the atmospheric model intercomparison project. J Clim 9:2727–2750

Sperber KR, Brankovic C, Deque M, Frederiksen CS, Graham R, Kitoh A, Kobayashi C, Palmer T, Puri K, Tennant W, Volodin E (2001) Dynamical seasonal predictability of the Asian summer monsoon. Mon Weather Rev 129:2226–2248

Sperber KR, Annamalai H, Kang I-S, Kitoh A, Moise A, Turner A, Wang B, Zhou T (2012) The Asian summer monsoon: an intercomparison of CMIP5 vs. CMIP3 simulations of the late 20th century. Clim Dyn. doi:10.1007/s00382-012-1607-6

Squires P, Twomey S (1961) The relation between cloud drop numbers and the spectrum of cloud nuclei. Phys Precip. Monograph, no. 5, pp 211–219, AGU, Washington, DC

Tao WK, Lang S, Olson WS, Meneghini R, Yang S, Simpson J, Kummerow C, Smith E, Halverson J (2001) Retrieved vertical profiles of latent heat release using TRMM rainfall products for february 1998. J Appl Meteorol 40:957–982

Tao W-K, Smith EA, Adler R, Haddad Z, Hou A, Kakar R, Krishnamurti T, Kummerow C, Lang S, Meneghini R, Olson W, Satoh S, Shige S, Simpson J, Takayabu Y, Tripoli G, Yang S (2006) Retrieval of latent heating from TRMM measurements. Bull Amer Meteor Soc 87:1555–1572

Tao W-K, Chen J-P, Li Z, Wang C, Zhang C (2012) Impact of aerosols on convective clouds and precipitation. Rev Geophys 50:RG2001. doi:10.1029/2011RG000369

Twomey S (1977) The influence of pollution on the shortwave albedo of clouds. J Atmos Sci 34:1149–1152

Twomey S, Piepgrass AM, Wolfe TL (1984) An assessment of the impact of pollution on global cloud albedo. Tellus 36B:356–366

Walcek CJ, Stockwell WR, Chang JS (1990) Theoretical estimates of the dynamic, radiative, and chemical effects of clouds on tropospheric trace gases. Atmos Res 25:53–69

Wang B, Ding Q, Fu X, Kang I-S, Jin K, Shukla J, Doblas-Reyes F (2005) Fundamental challenges in simulation and prediction of summer monsoon rainfall. Geophys Res Lett 32:L15711. doi:10.1029/2005GL02273412

Warner J (1968) A reduction in rainfall associated with smoke from sugar-cane fires: an inadvertent weather modification? J Appl Meteor 7:247–251

Warner J, Twomey S (1967) The production of cloud nuclei by cane fires and the effects on cloud droplet concentration. J Atmos Sci 24:704–706

Webster PJ, Magaña VO, Palmer TN, Shukla J, Tomas RA, Yanai M, Yasunari T (1998) Monsoons: processes, predictability, and the prospects for prediction. J Geophys Res 103:14451–14510

Xie S-P, Xu H, Saji NH, Wang Y (2006) Role of narrow mountains in large-scale organization of Asian monsoon convection. J Clim 19:3420–3429

Zhou YP, Tao W-K, Hou AY, Olson WS, Shie C-L, Lau K-M, Chou M-D, Lin X, Grecu M (2007) Use of high-resolution satellite observations to evaluate cloud and precipitation statistics from cloud-resolving model simulations. Part I: South China Sea monsoon experiment. J Atmos Sci 64:4309–4329